JOURNAL OF EXPERIMENTAL AND THEORETICAL PHYSICS, 2024, Vol. 165, No. 3, pp. 317–333

ATOMS, MOLECULES, OPTICS

DIFFRACTION RADIATION AT THE OPEN END OF A CIRCULAR WAVEGUIDE WITH DIELECTRIC FILLING

© 2024 S. N. Galyamin*

Saint Petersburg State University, 7/9 Universitetskaya nab., St. Petersburg, 199034 Russia

**e-mail: s.galyamin@spbu.ru*

Received October 12, 2023

Revised November 07, 2023

Accepted November 08, 2023

Abstract. An analytical solution to the canonical problem of diffraction radiation of a uniformly moving point charge at the open end of a circular waveguide with a uniform dielectric filling is presented. The case of motion along the axis is considered. A modified mode-matching method was used in the solution, leading to the Wiener–Hopf–Fock equation, and after its formal solution, to an infinite linear system of equations for the excitation coefficients of waveguide modes. This system is solved numerically by the reduction method with any given accuracy. Numerical results are obtained for the case of charge exit from the waveguide.

Keywords: *diffraction radiation*, *diffraction*, *uniformly moving charge*, *canonical problem*, *Wiener-Hopf technique*

DOI: 10.31857/S00444510240303e5

1. INTRODUCTION

Diffraction radiation is usually understood as radiation generated by a uniformly moving point charge (or other source) at various inhomogeneities which cannot be reduced to transition radiation or Vavilov–Cherenkov radiation [1]. From classical diffraction problems (the most characteristic of which are, for example, the diffraction of a plane wave on a half-plane, a round hole in a conductive screen or wedge, as well as the emission of a waveguide mode from the open end of a waveguide), this problem differs not in its mathematical essence, but only in a specific type of source that interacts with inhomogeneity with its Coulomb field (the latter can be decomposed into plane waves decreasing from the trajectory of the charge). However, historically, the situation has developed in such a way that, despite the commonality of tasks and methods of solution, the theory of diffraction radiation (DR) has developed quite isolated from the theory of diffraction, especially in recent decades, therefore a number of important diffraction problems with a moving source have not been considered so far.

The fundamentals of the theory of DR are described, for example, in fundamental reviews [1, 2], where ideally conducting inhomogeneities in vacuum were considered. In [1], the theory of DR is presented for a number of two-dimensional problems with a rigorous solution, the work [2] is devoted to the development of the scalar theory of DR. It is also worth mentioning a number of works where waveguide problems were considered [3 –5] and other methods for calculating the DR from complex inhomogeneities were developed [6 – 9].

However, in recent years, the importance of the theory of DR in the presence of dielectric inhomogeneities has increased significantly. In a certain sense, it all started with Vavilov–Cherenkov radiation in layered waveguides, which has been successfully used in the wakefield acceleration method of charged particles over the past decades [10 – 16]. A typical structure used is the so-called “capillary”, i.e. a dielectric tube with an axisymmetric vacuum channel (for passing charged particles) and a metal coating on the outside. The same capillaries that are used in the framework of wakefield acceleration,

as well as similar, but more multilayer structures, have been proposed to be used to generate narrow-band radiation (including in the terahertz range) [9, 17 –20]. At the same time, an important question arises of the effective output of the generated radiation from the waveguide into the open space, which, when formulated mathematically, leads to a family of problems in the theory of DR at the open end of a waveguide with dielectric filling.

As is known from the theory of diffraction on similar structures, the presence of a dielectric significantly complicates the problem: for example, infinite linear [21 –24] or nonlinear [25, 26] systems arise, and the solution is not constructed in a closed form. Perhaps for this reason, there is still no rigorous solution in the literature to a number of classical problems with dielectric inhomogeneity of the type described above (with the exception of a number of works by the author of this article [27, 26], where, however, "closed" geometry was considered), while similar vacuum structures were analyzed from various sides [3 –5].

This paper is devoted to the presentation of a rigorous analytical approach for the analysis of DR at the open end of a circular waveguide with layered dielectric filling, which eliminates the noted gap in the theory of DR (for clarity, the simplest case of continuous filling is considered). The idea of this method (using the example of waveguide mode diffraction) is presented in articles [21, 22] for plane-parallel geometry, while for cylindrical geometry this method was developed in our recent works [28, 29], although some of its elements are also contained in the article [30].

Finally, it should be noted that from the point of view of terminology, in this case it would probably be more correct to talk not only about DR, but about the combination of DR and transition radiation. However, the problem under consideration, both in terms of formulation and solution methods, is closest to the theory of diffraction, therefore we do not mention transition radiation either in the title or in the Introduction, but we will touch on this issue when discussing analytical results.

2. FORMULATION OF THE PROBLEM AND SOLUTION

We will solve the problem for the amplitudes of the Fourier harmonics of the desired fields (in fact, in the harmonic mode), i.e. we assume that the components of the field are decomposed into a Fourier integral of the form

$$H_\varphi = \int_{-\infty}^{+\infty} H_{\varphi\omega} e^{-i\omega t}\, d\omega = 2\mathrm{Re} \int_{0}^{+\infty} H_{\varphi\omega} e^{-i\omega t}\, d\omega, \tag{1}$$

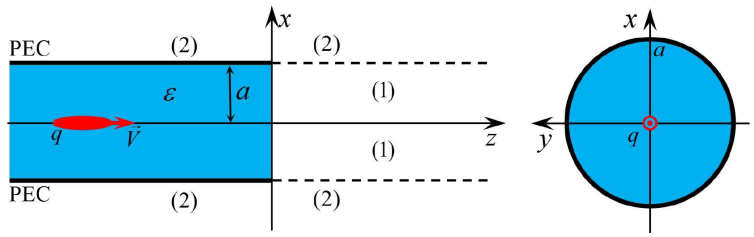

Fig. 1. Geometry of the problem and main designations

and it is necessary to find $H_{\varphi\omega}$ and similar amplitudes of the other components (a cylindrical coordinate system ρ,φ,z is used). Due to the second equality in (1), it is sufficient to assume that $\omega > 0$. A semi-infinite circular waveguide of radius a in vacuum filled with a dielectric with $\varepsilon > 1$ is considered (Fig. 1). A point charge q moves uniformly along the axis of the waveguide at a speed $\upsilon = c\beta$ (c — the speed of light in a vacuum). For the sake of certainty, we will assume that the Cherenkov condition is fulfilled, i. e. $\varepsilon\beta^2 > 1$, however, this assumption does not affect the structure of the general solution in any way.

The problem is axisymmetric, so outside the source, the remaining nonzero components of the field are expressed as follows:

$$E_{\rho\omega} = \frac{1}{ik_0\varepsilon}\frac{\partial H_{\varphi\omega}}{\partial z}, \quad E_{z\omega} = \frac{i}{k_0\varepsilon\rho}\left(H_{\varphi\omega} + \rho\frac{\partial H_{\varphi\omega}}{\partial\rho}\right), \tag{2}$$

where $k_0 = \omega / c + i\delta$ ($\delta \to +0$, i.e., the presence of a small positive imaginary part of k_0 is assumed, which can be interpreted as the introduction of a small attenuation into a vacuum).

The incident field inside the waveguide ($\rho < a$, $z < 0$) has the form

$$H^{(i)}_{\varphi\omega} = \frac{iqs}{2c}e^{i\frac{\omega}{\upsilon}z}\left[H^{(1)}_1(\rho s) - \frac{H^{(1)}_0(as)}{J_0(as)}J_1(\rho s)\right], \tag{3}$$

where

$$s = \sqrt{k_0^2 / \beta^2(\varepsilon\beta^2 - 1)}, \quad \mathrm{Im}s > 0.$$

The incident field in a vacuum is set everywhere outside the waveguide, it has the form

$$H^{(i0)}_{\varphi\omega} = \frac{iqs_0}{2c}e^{i\frac{\omega}{\upsilon}z}H^{(1)}_1(\rho s_0), \tag{4}$$

where

$$s_0 = i\sigma_0, \quad \sigma_0 = k_0\sqrt{\beta^{-2} - 1}, \quad \mathrm{Re}\sigma_0 > 0.$$

The field reflected back into the waveguide has the form

$$H^{(r)}_{\varphi\omega} = \frac{iq}{2c}\sum_{m=1}^{\infty}M_m J_1\left(\frac{\rho j_{0m}}{a}\right)e^{-ik_{zm}z}, \tag{5}$$

where j_{0m} — are the zeros of the Bessel function $J_0(\xi)$,

$$k_{zm} = \sqrt{k_0^2\varepsilon - \frac{j_{0m}^2}{a^2}}, \quad \mathrm{Im}k_{zm} > 0. \tag{6}$$

The coefficients $\{M_m\}$ need to be found. However, from the Meixner condition on the edge $\rho = a - 0$, $z = -0$ it is possible to determine the behavior of these coefficients for large numbers [25- 29]:

$$M_m \sim m^{-(1+\tau)} \quad \text{at} \quad m \to \infty, \qquad \tau = \frac{1}{\pi}\mathrm{asin}\frac{\varepsilon - 1}{2(\varepsilon + 1)}, \tag{7}$$

with $0 < \tau < 1 / 6$.

The further course of the solution is similar to the work [28]. Diffraction field in vacuum (regions “1” and “2”, see Fig. 1) is described by the Helmholtz equation:

$$\left[\partial^2 / \partial z^2 + \partial^2 / \partial\rho^2 + \rho^{-1}\partial / \partial\rho + \left(k_0^2 - \rho^{-2}\right)\right]H^{(1,2)}_{\varphi\omega} = 0. \tag{8}$$

We introduce into consideration functions $\Psi_{\pm}(\rho,\alpha)$ that are essentially one-sided Fourier transforms of the field $H_{\varphi\omega}$ (hereafter, the subscript $\pm$ means that the function is holomorphic and has no zeros, respectively, in the upper half-plane, $\mathrm{Im}\,\alpha > -\delta$, or in the lower half-plane, $\mathrm{Im}\,\alpha < \delta$):

$$\Psi_{+}^{(1,2)}(\rho,\alpha) = (2\pi)^{-1}\int_{0}^{\infty} dz H_{\varphi\omega}^{(1,2)}(\rho,z)e^{i\alpha z}, \tag{9}$$

$$\Psi_{-}^{(2}(\rho,\alpha) = (2\pi)^{-1}\int_{-\infty}^{0} dz H_{\varphi\omega}^{(2)}(\rho,z)e^{i\alpha z}, \tag{10}$$

and similar Fourier transforms of the field $E_{z\omega}^{(1,2)}$, for example

$$\Phi_{+}^{(1,2)}(\rho,\alpha) = (2\pi)^{-1}\int_{0}^{\infty} dz \frac{k_0}{i} E_{z\omega}^{(1,2)}(\rho,z)e^{i\alpha z}. \tag{11}$$

Further transformations are described in detail in the article [28], so here we give them schematically. In the domain "1" ($\rho < a, z > 0$) we apply the one-sided transformation (9) to (8) and obtain an inhomogeneous differential equation for a function $\Psi_{+}^{(1)}(\rho,\alpha)$, in the left-hand part of which there is a Bessel operator, and the right-hand part is determined by the values $\partial H_{\varphi\omega} / \partial z\Big|_{z=0}$ and $H_{\varphi\omega}\Big|_{z=0}$ and is found from the boundary conditions of continuity of the tangential components of the field in the cross-section $z = 0$. In domain "2" ($\rho > a, -\infty < z < +\infty$) we apply the usual Fourier transform to (8), representing it as the sum of (9) and (10), and obtain a homogeneous Bessel equation for the function $\Psi_{-}^{(2)}(\rho,\alpha) + \Psi_{+}^{(2)}(\rho,\alpha)$. The general solutions of these equations have the following form:

$$\Psi_{+}^{(1)}(\rho,\alpha) = C_1 J_1(\rho\kappa) + D_1 H_1^{(1)}(\rho\kappa) + \tilde{\Psi}_{p}^{(1)}(\rho,\alpha), \tag{12}$$

$$\Psi_{-}^{(2)}(\rho,\alpha) + \Psi_{+}^{(2)}(\rho,\alpha) = C_2 H_1^{(1)}(\rho\kappa), \tag{13}$$

$$\begin{aligned}\tilde{\Psi}_{p}^{(1)}(\rho,\alpha) = \frac{i}{2\pi}\frac{iq}{2c}\Bigg[&\frac{\omega / (\upsilon\varepsilon) - \alpha}{\kappa^2 - s^2} s \times \\ &\times\left(H_1^{(1)}(\rho s) - \frac{H_0^{(1)}(as)}{J_0(as)} J_1(\rho s)\right) - \\ -\frac{s_0}{\omega / \upsilon + \alpha} H_1^{(1)}(\rho s_0) &- \sum_{m=1}^{\infty} M_m \frac{k_{zm} / \varepsilon + \alpha}{\alpha_m^2 - \alpha^2} J_1\left(\frac{\rho j_{0m}}{a}\right)\Bigg]\end{aligned} \tag{14}$$

where $C_{1,2}$, D_1 are some constants that will be defined below,

$$\alpha_m = \sqrt{k_0^2 - \frac{j_{0m}^2}{a^2}}, \quad \operatorname{Im}\alpha_m > 0, \tag{15}$$

— longitudinal wave numbers of a vacuum waveguide of radius a.

Note that the fundamental point for constructing a correct solution is the presence of a summand $D_1 H_1^{(1)}(\rho\kappa)$ in the general solution (12). Recall that $\Psi_{+}^{(1)}(\rho,\alpha)$ is a transformation of the diffraction field in the vacuum region, i.e. it corresponds to the solution of *homogeneous* Maxwell equations. The particular solution (14) contains functions singular on the axis (taking into account the difference in the incident field to the left and right of the boundary $z = 0$), this singularity at $\rho = 0$ should be compensated by the selection of a constant D_1. This circumstance is atypical, since usually only regular solutions, i.e. Bessel functions, are taken as solutions of the homogeneous Bessel equation in the region containing the zero point.

So, the singularity at $\rho \to 0$ in (12) will be compensated when choosing

$$D_1 = \frac{-i}{2\pi}\frac{iq}{2c}\kappa\left(\frac{\omega/(\upsilon\varepsilon)-\alpha}{\kappa^2-s^2}-\frac{1}{\omega/\upsilon+\alpha}\right), \tag{16}$$

therefore, you can rewrite

$$\Psi_+^{(1)}(\rho,\alpha) = C_1 J_1(\rho\kappa) + \Psi_p^{(1)}(\rho,\alpha), \tag{17}$$

where

$$\Psi_p^{(1)}(\rho,\alpha) = \frac{i}{2\pi}\frac{iq}{2c}\left[\begin{array}{c}\dfrac{\omega/(\upsilon\varepsilon)-\alpha}{\kappa^2-s^2}\left(\begin{array}{c}sH_1^{(1)}(\rho s)-\kappa H_1^{(1)}(\rho\kappa)-\\ -s\dfrac{H_0^{(1)}(as)}{J_0(as)}J_1(\rho s)\end{array}\right)-\\ -\dfrac{1}{\omega/\upsilon+\alpha}\left(s_0H_1^{(1)}(\rho s_0)-\kappa H_1^{(1)}(\rho\kappa)\right)-\\ \sum\limits_{m=1}^{\infty}M_m\dfrac{k_{zm}/\varepsilon+\alpha}{\alpha_m^2-\alpha^2}J_1\left(\dfrac{\rho j_{0m}}{a}\right)\end{array}\right] \tag{18}$$

Similarly

$$\Phi_+^{(1)}(\rho,\alpha) = C_1\frac{i\kappa}{k_0}J_0(\rho\kappa) + \Phi_p^{(1)}(\rho,\alpha), \tag{19}$$

$$\Phi_-^{(2)}(\rho,\alpha) + \Phi_+^{(2)}(\rho,\alpha) = C_2\frac{i\kappa}{k_0}H_0^{(1)}(\rho\kappa), \tag{20}$$

$$\Phi_p^{(1)}(\rho,\alpha) = \frac{i}{2\pi}\frac{i}{k_0}\frac{iq}{2c}\left[\begin{array}{c}\dfrac{\omega/(\upsilon\varepsilon)-\alpha}{\kappa^2-s^2}\left(\begin{array}{c}s^2H_0^{(1)}(\rho s)-\kappa^2H_0^{(1)}(\rho\kappa)-\\ -s^2\dfrac{H_0^{(1)}(as)}{J_0(as)}J_0(\rho s)\end{array}\right)-\\ -\dfrac{1}{\omega/\upsilon+\alpha}\left(s_0^2H_0^{(1)}(\rho s_0)-\kappa^2H_0^{(1)}(\rho\kappa)\right)-\\ \sum\limits_{m=1}^{\infty}M_m\dfrac{j_{0m}}{a}\dfrac{k_{zm}/\varepsilon+\alpha}{\alpha_m^2-\alpha^2}J_0\left(\dfrac{\rho j_{0m}}{a}\right)\end{array}\right] \tag{21}$$

From the condition $E_{z\omega}^{(2)} = 0$ at $\rho = a$, $z < 0$ we get

$$C_2 = \frac{\Phi_+^{(2)}(a,\alpha) + \dfrac{i}{2\pi}\dfrac{iq}{2c}\dfrac{i}{k_0}\dfrac{s_0^2H_0^{(1)}(as_0)}{\alpha+\omega\upsilon^{-1}-i0}}{i\kappa k_0^{-1}H_0^{(1)}(a\kappa)}. \tag{22}$$

Stitching $E_{z\omega}$ at $\rho = a$, $z > 0$, we get

$$C_1 = \frac{\Phi_+^{(2)}(a,\alpha) - \Phi_p^{(1)}(a,\alpha)}{i\kappa k_0^{-1}J_0(a\kappa)}. \tag{23}$$

Next, by stitching $H_{\varphi\omega}$ at $\rho = a$, $z > 0$ and using (23) and (21), we obtain the connection

$$\Psi_+^{(2)}(a,\alpha) = \frac{k_0}{i}\frac{\Phi_+^{(2)}(a,\alpha)J_1(a\kappa)}{\kappa J_0(a\kappa)} + \frac{i}{2\pi}\frac{iq}{2c}\frac{1}{J_0(a\kappa)}\times$$
$$\times\left[\begin{array}{c}\dfrac{2i}{a\pi}\dfrac{\omega/(\upsilon\varepsilon)-\alpha}{\kappa^2-s^2}\dfrac{J_0(as)-J_0(a\kappa)}{J_0(as)}+\\ +\dfrac{s_0}{\omega\upsilon^{-1}+\alpha}\left(\begin{array}{c}\dfrac{s_0}{\kappa}H_0^{(1)}(as_0)J_1(a\kappa)-\\ -J_0(a\kappa)H_1^{(1)}(as_0)-\dfrac{2i}{\pi as_0}\end{array}\right)\end{array}\right] \tag{24}$$
$$-\frac{i}{2\pi}\frac{iq}{2c}\sum_{m=1}^{\infty}M_m J_1(j_{0m})\frac{k_{zm}/\varepsilon+\alpha}{\alpha_m^2-\alpha^2}.$$

It is easy to see that the right-hand side in (24) has no branching points, and also has no poles at the zeros of the denominators $\omega\upsilon^{-1}+\alpha$ and $\kappa^2 - s^2$. However, formally, it has "parasitic" poles at $\alpha = \alpha_p$, $p = 1,2,\ldots$, which must be compensated by imposing the so-called "regularizing relations" on the function $\Phi_+^{(2)}(a,\alpha)$ (see [28]):

$$\frac{k_0}{i}\Phi_+^{(2)}(a,\alpha_p) + \frac{i}{2\pi}\frac{iq}{2c}\frac{1}{J_1(j_{0p})}\times$$
$$\times\left[\frac{j_{0p}}{a}\left(\begin{array}{c}\dfrac{2i}{a\pi}\dfrac{\omega/(\upsilon\varepsilon)-\alpha_p}{\left(j_{0p}/a\right)^2-s^2}+\dfrac{1}{\omega/\upsilon+\alpha_p}\times\\ \times\left(\dfrac{s_0^2 a}{j_{0p}}J_1(j_{0p})H_0^{(1)}(as_0)-\dfrac{2i}{a\pi}\right)\end{array}\right)+\right] = 0, \tag{25}$$
$$+\frac{M_p a}{2}\left(\frac{k_{zp}}{\varepsilon}+\alpha_p\right)J_1^2(j_{0p})\Bigg]$$
$$p = 1,2,\ldots$$

Now, substituting (22) into (13) and using the connection (24), we obtain the Wiener–Hopf–Fock equation:

$$\Psi_-^{(2)}(a,\alpha) + \frac{2k_0\Phi_+^{(2)}(a,\alpha)}{\kappa G(\alpha)} + \frac{i}{2\pi}\frac{iq}{2c}\frac{1}{J_0(a\kappa)}\times$$
$$\times\left[\begin{array}{c}\dfrac{2i}{a\pi}\dfrac{\omega/(\upsilon\varepsilon)-\alpha}{\kappa^2-s^2}\dfrac{J_0(as)-J_0(a\kappa)}{J_0(as)}+\dfrac{s_0}{\omega/\upsilon+\alpha}\times\\ \times\left(\dfrac{s_0}{\kappa}H_0^{(1)}(as_0)J_1(a\kappa)-J_0(a\kappa)H_1^{(1)}(as_0)-\dfrac{2i}{as_0\pi}\right)\end{array}\right]- \tag{26}$$
$$-\frac{i}{2\pi}\frac{iq}{2c}\sum_{m=1}^{\infty}M_m J_1(j_{0m})\frac{k_{zm}/\varepsilon+\alpha}{\alpha_m^2-\alpha^2}-$$
$$-\frac{i}{2\pi}\frac{iq}{2c}\frac{s_0^2 H_0^{(1)}(as_0)H_1^{(1)}(a\kappa)}{\kappa H_0^{(1)}(a\kappa)(\alpha+\omega\upsilon^{-1}-i0)} = 0,$$

where

$$G(\alpha) = \pi a \kappa J_0(a\kappa) H_0^{(1)}(a\kappa).$$

By performing standard factorizations and asymptotic estimates, we obtain a formal solution to the equation (26) in the following form:

$$\Phi_+^{(2)}(a,\alpha) = \frac{i}{2\pi}\frac{iq}{2c}\frac{\kappa_+(\alpha)G_+(\alpha)}{2k_0}\times$$
$$\times\left[\begin{array}{c}\sum\limits_{m=1}^{\infty}\left(M_m J_1(j_{0m})U_{m+}(\alpha)+V_{m+}(\alpha)\right)-\\ -s_0^2 H_0^{(1)}(as_0)T_+(\alpha)\end{array}\right], \tag{27}$$

where

$$\kappa_\pm = \sqrt{k_0 \pm \alpha}, \quad G(\alpha) = G_+(\alpha)G_-(\alpha)$$

(standart integral formulas from [25] can be used for calculation of $G_\pm(\alpha)$),

$$U_{m+}(\alpha) = G_+(\alpha_m)\kappa_+(\alpha_m)\frac{k_{zm}/\varepsilon - \alpha_m}{2\alpha_m(\alpha_m+\alpha)}, \tag{28}$$

$$V_{m+}(\alpha) = \frac{2i}{a\pi}\frac{G_+(\alpha_m)\kappa_+(\alpha_m)j_{0m}}{a^2\alpha_m J_1(j_{0m})(\alpha_m+\alpha)}\times$$
$$\times\left(\frac{\omega/(\upsilon\varepsilon)+\alpha_m}{\left(j_{0m}/a\right)^2 - s^2} + \frac{1}{\alpha_m - \dfrac{\omega}{\upsilon}}\right), \tag{29}$$

$$T_+(\alpha) = \frac{2i}{\alpha+\omega/\upsilon - i0}\times$$
$$\times\left[\frac{1}{G_+(\alpha)\kappa_+(\alpha)} - \frac{1}{G_+(-\omega/\upsilon)\kappa_+(-\omega/\upsilon)}\right]. \tag{30}$$

Substituting solution (27) into condition (25), we obtain an infinite linear system of equations for the desired coefficients $\{M_m\}$:

$$\sum_{m=1}^{\infty} W_{pm}M_m = w_p, \quad p = 1,2,\ldots, \tag{31}$$

where

$$W_{pm} = J_1(j_{0m})\left[\begin{array}{c}\kappa_+(\alpha_p)G_+(\alpha_p)U_{m+}(\alpha_p)+\\ +\delta_{mp}ia\left(\dfrac{k_{zm}}{\varepsilon}+\alpha_m\right)\end{array}\right],$$

$$w_p = \frac{-2ij_{0p}}{aJ_1(j_{0p})}\left[\begin{array}{c}\dfrac{2i}{\pi a}\dfrac{\omega/(\upsilon\varepsilon)-\alpha_p}{\left(j_{0p}/a\right)^2 - s^2}+\\ +\dfrac{1}{\alpha_p+\omega/\upsilon}\left(\dfrac{s_0^2 a}{j_{0p}}J_1(j_{0p})H_0^{(1)}(as_0) - \dfrac{2i}{a\pi}\right)\end{array}\right] - \tag{32}$$
$$-\kappa_+(\alpha_p)G_+(\alpha_p)\left[\sum_{m=1}^{\infty}V_{m+}(\alpha_p) + is_0^2 H_0^{(1)}(as_0)T_+(\alpha_p)\right],$$

where δ_{mp} is the Kronecker symbol. As can be shown, this system converges and can be solved numerically by the reduction method (similar to how a similar system was solved in [28]), as a result of which the set of coefficients $\{M_m\}$ can be considered known. After that, it is not difficult to calculate the field outside the waveguide.

In particular, for the domain $z > 0$ we have the following unified representation for all ρ (the corresponding transformations are similar to the transformations in [28] and are quite cumbersome, so we do not give them here):

$$H_{\varphi\omega}^{(1,2)}(\rho,z>0) = \frac{i}{2\pi}\frac{iq}{2c}\sum_{m=1}^{\infty}\frac{\kappa_+(\alpha_m)G_+(\alpha_m)}{\alpha_m}\times$$
$$\times Q_m 2\pi a L_m^+(\rho,z) + \frac{i}{2\pi}\frac{iq}{2c}\frac{s_0^2 H_0^{(1)}(as_0)}{G_+(-\omega/\upsilon)\kappa_+(-\omega/\upsilon)}2\pi a L_\beta^+(\rho,z). \tag{33}$$

Here

$$Q_m = \frac{1}{2i}\left[\times\left[\begin{array}{c}\dfrac{2i}{\pi a}\dfrac{j_{0m}}{a^2 J_1(j_{0m})}\times \\ \left(\dfrac{\omega/(\upsilon\varepsilon)+\alpha_m}{\left(j_{0m}/a\right)^2 - s^2} + \dfrac{1}{\alpha_m - \omega/\upsilon}\right) + \\ + M_m J_1(j_{0m})\dfrac{k_{zm}/\varepsilon - \alpha_m}{2}\end{array}\right] + \right]. \tag{34}$$

The function L_m^+ has the form (its definition coincides with formula (47) in [28]):

$$L_m^+(\rho,z) = \int\limits_{-\Gamma_+'}\frac{\kappa(\alpha)J_1(\rho\kappa)J_0(a\kappa)}{\kappa_+(\alpha)G_+(\alpha)(\alpha-\alpha_m)}e^{i\alpha z}\,d\alpha, \tag{35}$$

where the contour $-\Gamma_+'$ goes from a point k_0 along the branch cut of the function $\kappa(\alpha)$ in the first quadrant along the shore with $\arg\kappa = 0$. The following parameterization is valid for this contour:

$$\alpha = k_0' k_0''/\alpha'' + i\alpha'', \quad \alpha'' \in [k_0'', \infty).$$

The function L_β^+ differs from the L_m^+ by replacement $\alpha_m \to \omega/\upsilon$ and looks like

$$L_\beta^+(\rho,z) = \int\limits_{-\Gamma_+'}\frac{\kappa(\alpha)J_1(\rho\kappa)J_0(a\kappa)}{\kappa_+(\alpha)G_+(\alpha)(\alpha-\omega/\upsilon)}e^{i\alpha z}\,d\alpha. \tag{36}$$

For asymptotic field analysis, the following representation is more convenient for a field in the domain "2" ($\rho > a$, $-\infty < z < \infty$) with integrals along the real axis α:

$$H_{\varphi\omega}^{(2)}(\rho,z) = \frac{i}{2\pi}\frac{iq}{2c}\sum_{m=1}^{\infty}\frac{\kappa_+(\alpha_m)G_+(\alpha_m)}{\alpha_m}Q_m I_m^{(2)}(\rho,z) +$$
$$+\frac{i}{2\pi}\frac{iq}{2c}\frac{s_0^2 H_0^{(1)}(as_0)}{G_+(-\omega/\upsilon)\kappa_+(-\omega/\upsilon)}I_\beta^{(2)}(\rho,z), \tag{37}$$

where

$$I_m^{(2)}(\rho,z) = \int\limits_{-\infty}^{+\infty}\frac{\kappa_+(\alpha)G_+(\alpha)H_1^{(1)}(\rho\kappa)}{\kappa(\alpha)H_0^{(1)}(a\kappa)(\alpha+\alpha_m)}e^{-i\alpha z}\,d\alpha, \tag{38}$$

$$I_\beta^{(2)}(\rho,z) = \int\limits_{-\infty}^{+\infty}\frac{\kappa_+(\alpha)G_+(\alpha)H_1^{(1)}(\rho\kappa)}{\kappa(\alpha)H_0^{(1)}(a\kappa)(\alpha+\omega/\upsilon-i0)}e^{-i\alpha z}\,d\alpha. \tag{39}$$

The second term in (33) and (37) describes diffraction radiation when a charge escapes from the open end of a vacuum waveguide. In particular, the second term in (37) will coincide with the corresponding expression in [4] (taking into account the obvious redesignations). The first term in (33) and (37) (the sum over m) is due to the presence of a vacuum-dielectric interface at the end of the waveguide, therefore it can be interpreted as transition radiation at the interface of a finite size bounded by the walls of the waveguide. Note also that the above solution is valid for the case of charge escape from the waveguide ($\upsilon > 0$, Fig. 1), and for the case of flight ($\upsilon < 0$), however, only the case $\upsilon > 0$ is discussed later.

We will discuss the procedure for the asmyptotic calculation of the field in the far-field zone (in the region "2") using the steepest descent method [32]. Let 's place the $x = y = z = 0$ point to the beginning of the spherical coordinate system R,θ,φ, the angle θ will be counted from the positive direction of the axis z. The asymptotics of the integral (38) were investigated in [28]. As usual, we assume that the inequalities defining the far-field zone are fulfilled: $k_0 R \gg 1$, as well as $R \gg a$ and the viewing angle θ lie in the range $\theta \gg \theta_{\min}$, $\pi - \theta \gg \theta_{\min}$, where $\theta_{\min} = 1 / \sqrt{k_0 R}$ (note that everywhere in the future it is assumed that $1 / \sqrt{k_0 R} > a / R$, , i.e., the minimum and maximum viewing angles always lie in the region "2").

The main term of the asymptotic integral (38) has the form of a spherical wave:

$$I_m^{(2)}(\rho,z) \approx \pi a \frac{\exp(ik_0 R)}{R} \frac{\kappa_-(k_0\cos\theta)}{G_+(k_0\cos\theta)} \frac{2J_0(ak_0\sin\theta)}{k_0\cos\theta - \alpha_m}. \tag{40}$$

The asymptotics of the integral (39) are constructed in a generally similar way. Note that the contribution of the pole $\alpha = -\omega / \upsilon + i0$ is exponentially small at β far from 1, so it is usually not taken into account in the main term [33]. However, for $\beta \to 1$ contribution of this pole ceases to be negligible in the general case, in addition, at small viewing angles, θ it is located near the saddle point. Taking into account this fact, the asymptotics (39) has the following form (see [32]):

$$\begin{aligned} I_\beta^{(2)}(\rho,z) \approx I_\beta^{(2)P}(\rho,z)\Phi(\theta-\theta_\beta) + \pi a \times \frac{\exp(ik_0 R)}{R} \times \\ \times \left[\frac{\kappa_-(k_0\cos\theta)}{G_+(k_0\cos\theta)} \frac{2J_0(ak_0\sin\theta)}{k_0\cos\theta - \omega/\upsilon} - \right. \\ \left. - \frac{\sqrt{\kappa(\omega/\upsilon)}}{\sqrt{k_0\sin\theta}} \frac{\sqrt{2}J_0\left(a\kappa(\omega/\upsilon)\right)}{b_0(\theta)G_+(\omega/\upsilon)\kappa_+(\omega/\upsilon)} \right] \pm \\ \pm \pi a \frac{\exp\left(ik_0 R - i(3\pi/4)\right)}{\sqrt{R\sin\theta}} 2iQ\left(\mp i\sqrt{k_0 R e^{i\frac{\pi}{4}}} b_0(\theta) \right) \times \\ \times \exp\left[-ik_0 R b_0^2(\theta)\right] \frac{\sqrt{2\kappa(\omega/\upsilon)}J_0\left(a\kappa(\omega/\upsilon)\right)}{G_+(\omega/\upsilon)\kappa_+(\omega/\upsilon)}, \end{aligned} \tag{41}$$

where $\Phi(\theta)$ is the Heaviside step function, the angle θ_β is determined by equality $\cos\theta_\beta = \beta$ or equality $\sin\theta_\beta = \gamma^{-1}$ ($\gamma = 1 / \sqrt{1-\beta^2}$ — Lorentz factor), the residue in the pole $\alpha = -\omega / \upsilon + i0$, denoted as $I_\beta^{(2)P}(\rho,z)$, is related to the incident field outside the waveguide (4) by the expression

$$\frac{i}{2\pi}\frac{iq}{2c}\frac{s_0^2 H_0^{(1)}(as_0)}{G_+(-\omega/\upsilon)\kappa_+(-\omega/\upsilon)} I_\beta^{(2)P}(\rho,z) = -H_{\varphi\omega}^{(i0)}(\rho,z), \tag{42}$$

$$\begin{gathered} b_0(\theta) = \sqrt{1-\sin(\theta+\theta_0)}, \\ \theta_0 = \pi/2 - i\operatorname{arcch}(\beta^{-1}), \\ \operatorname{Re} b_0 < 0, \end{gathered} \tag{43}$$

the signs $\pm$ correspond to $\arg b_0 \lessgtr 3\pi / 4$,

$$Q(y) = \int_y^\infty \exp(-\xi^2)d\xi = e^{-y^2}\int_0^\infty \exp(-\xi^2 - 2\xi y)d\xi. \tag{44}$$

The first term in (41), according to equalities (37) and (42), compensates the incident field $H_{\varphi\omega}^{(i0)}(\rho,z)$ in the area of angles $\theta > \theta_\beta$. Thus, the eigenfield of the charge outside the waveguide turns out to be concentrated inside a cone $\theta < \theta_\beta$, the spanning angle of which decreases with an increase in the Lorentz factor γ, $\theta_\beta \sim 1/\gamma$ at $\gamma \gg 1$. However, the boundaries of this cone are not sharp, since the uniform asymptotic formula (41) describes a smooth transition from the presence of a pole contribution to its absence. Also, since the first term under discussion in expression (41) is proportional to the incident field $H_{\varphi\omega}^{(i0)}(\rho,z)$, this asymptotic must be considered together with the incident field. It is useful to introduce the appropriate value $I^{(i0)}(\rho,z)$ according to the equality

$$H_{\varphi\omega}^{(i0)}(\rho,z) = \frac{i}{2\pi}\frac{iq}{2c}\frac{s_0^2 H_0^{(1)}(as_0)}{G_+(-\omega/\upsilon)\kappa_+(-\omega/\upsilon)} I^{(i0)}(\rho,z). \tag{45}$$

Then the sum $I^{(i0)}(\rho,z) + I_\beta^{(2)}(\rho,z)$ is proportional to the total field in the region "2" in the case of charge exit from the open end of the vacuum waveguide and, taking into account the uniform asymptotics (41) for the second term, describes a smooth transition from the presence of its own charge field inside the cone $\theta < \theta_\beta$ to its absence outside this cone.

When the $\beta \to 1$ first term in square brackets in (41) has a singularity at $\theta \to 0$ (the pole approaches the saddle point), this peculiarity is compensated by the second term in square brackets, and in general the square bracket is always finite. The jump of the first term in (41) at $\theta = \theta_\beta$, associated with the "switching on" of the Heaviside function at $\theta > \theta_\beta$, is compensated by a jump in the last term, since when passing θ through the value θ_β the pole $\alpha = -\omega/\upsilon + i0$ crosses the contour of the steepest descent, $\arg b_0(\theta)$ passes through the value $3\pi/4$ and the value of the function $Q(y)$ changes by a jump, the value of which is determined by the expression

$$Q(y) + Q(-y) = \sqrt{\pi}.$$

In case when the pole is far from the saddle point, i.e. when the angle θ satisfies the inequality

$$|\sqrt{k_0 R}b_0(\theta)| \gg 1,$$

we have

$$\pm 2iQ\left(\mp i\sqrt{k_0 R}e^{i\frac{\pi}{4}}b_0(\theta)\right)\exp\left[-ik_0 R b_0^2(\theta)\right] \approx \frac{-\exp(-i\pi/4)}{\sqrt{k_0 R}b_0(\theta)}, \tag{46}$$

and the asymptotics takes a simpler form (i.e. it goes into the usual "non-uniform" asymptotics):

$$I_\beta^{(2)}(\rho,z) \approx I_\beta^{(2)P}(\rho,z)\Phi(\theta-\theta_\beta) + \\ + \pi a\frac{\exp(ik_0 R)}{R}\frac{\kappa_-(k_0\cos\theta)}{G_+(k_0\cos\theta)}\frac{2J_0(ak_0\sin\theta)}{k_0\cos\theta - \omega/\upsilon}, \tag{47}$$

where the second term is similar in form to expression (40) and describes a spherical wave of diffraction radiation.

We will discuss in more detail the condition of sufficient distance of the pole from the saddle point, which we will write as

$$\left|\sqrt{k_0 R} b_0(\theta)\right| = \sqrt{\Lambda},$$

where Λ is some "large" number. After simple transformations, we have

$$\left|\sqrt{k_0 R} b_0(\theta)\right| = \sqrt{k_0 R}\sqrt{\beta^{-1} - \cos\theta} = \sqrt{\Lambda}. \quad (48)$$

At the viewing angle $\theta = \theta_\beta$ condition (48) gives

$$k_0 R = \Lambda \beta \gamma^2,$$

that at $\gamma \gg 1$ transforms into

$$k_0 R \approx \Lambda \gamma^2.$$

With a minimum viewing angle

$$\theta = \theta_{\min} = 1/\sqrt{k_0 R}, \quad k_0 R \gg 1,$$

condition (48) gives

$$k_0 R = \frac{\Lambda - 1/2}{\beta^{-1} - 1},$$

that at $\gamma \gg 1$ transforms into

$$k_0 R \approx (2\Lambda - 1)\gamma^2.$$

The asymptotics of the function $Q(y)$, following from (46) works quite well already at $\Lambda = 10$. Therefore, with this value of Λ and $\gamma \gg 1$ the use of "non-uniform" asymptotics (47) for $\theta = \theta_\beta$ is justified at distances $R \geq 10\gamma^2 / k_0$, while at $\theta = 1/\sqrt{k_0 R}$ (i.e., at a minimum angle) it is justified at distances $R \geq 19\gamma^2 / k_0$, i.e. starting from almost twice the distance. It also follows from (48) that if "non-uniform" asymptotics is applicable at the corresponding R, for example, at $\theta = \theta_\beta$, then it is also applicable for all others θ ($|b_0(\theta)|$ increases monotonously with the growth of θ). For $\theta \sim \theta_\beta$ using "non-uniform" asymptotics is unjustified at $\Lambda < 10$, as will be illustrated below.

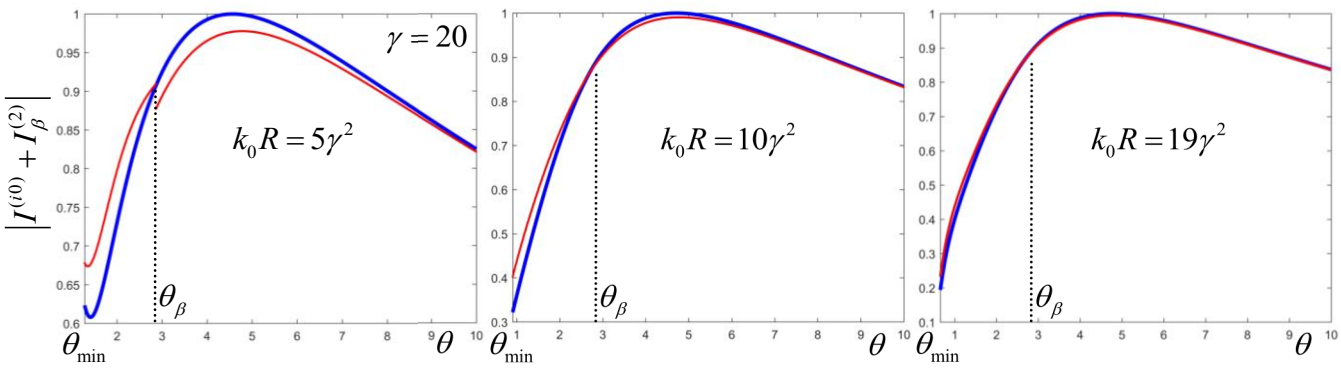

Fig. 2. (In color online) The Fourier harmonic modulus of the full field (for the case of charge departure from a vacuum waveguide) in the far-field zone of the region "2" at small angles $\theta \sim \theta_\beta$, the value of the Lorentz factor $\gamma = 20$ and various distances R at the first Cherenkov frequency, $\omega = \omega_1^{CR}$. The blue line is calculated according to the formula of uniform asymptotics (41), the red line is calculated according to the formula of "non-uniform" asymptotics (47). Each graph is normalized to the maximum of the blue curve. Problem parameters: $a = 0.24$ cm, $\varepsilon = 2 + 0.001i$, $q = -1$nC $\omega_1^{CR} \approx 2\pi \cdot 47.8$ GHz

3. NUMERICAL RESULTS

Within the framework of modern practical applications of the waveguide structure under consideration, the generation of Vavilov–Cherenkov radiation (VCR) by relativistic electron bunches in a waveguide (in the form of a discrete set of so-called Cherenkov modes) and its output from the open end into free space is of the greatest interest. It should be noted that in recent years, experiments on the registration of an VCR in a fairly narrow spectral range have been typical. For example,

in [34] the VCR spectrum was measured in the wavelength range 0.8-1.6cm, in [35] an ultra-narrowband VCR in the far infrared range with a relative spectral band width of the order of $10^{-4} - 10^{-5}$ was studied, in [36] the results of the registration of an VCR at a wavelength of 600 nm with a band width of 10nm are presented. Therefore, bearing in mind such narrow-band measurements, in this paper we will limit ourselves to analyzing the Fourier harmonics of the field. Relativistic charge velocities will also be considered in the future, and the corresponding Cherenkov frequencies will be mainly used to obtain graphical results for Fourier harmonics of the field.

For a given charge velocity β (or for a given Lorentz factor γ) the frequency of the "Cherenkov mode" f_l^{CR} (l is the mode number) is determined from the known expression

$$\omega_l^{\mathrm{CR}} = 2\pi f_l^{\mathrm{CR}} = c\beta j_{0l} / (a\sqrt{\varepsilon\beta^2 - 1}), \tag{49}$$

where j_{0l} is the l zero of the Bessel function $J_0(\xi)$. The expression (49) means that $k_{zl} = \omega_l^{\mathrm{CR}} / \upsilon$, i.e., the l waveguide mode is synchronous with the charge, while equality $as = j_{0l}$ is also fulfilled.

At this frequency, generally speaking, the incident field inside the waveguide (3) is equal to infinity due to the presence $J_0(as)$ in the denominator, which is also reflected in the final formulas (32) and (34), where there is an expression in the denominator $j_{0m}^2 a^{-2} - s^2$ that also vanishes. Therefore, we proceed as follows: we introduce a small absorption into the dielectric, i.e. we suppose that

$$\varepsilon = \varepsilon' + i\varepsilon'', \quad \varepsilon'' > 0\,(\omega > 0), \quad \varepsilon'' \ll \varepsilon'.$$

The Cherenkov frequency, calculated by the formula (49) with such ε, also becomes a complex quantity with a small negative imaginary part. Further calculations are performed at the frequency $\omega = \mathrm{Re}\,\omega_l^{\mathrm{CR}}$, at which the incident field (3) and the corresponding terms in formulas (34) and (32) are finite, but have sharp maxima. Thus, the frequency spectrum of transition radiation at the considered interface of finite size (the first term in (33) and (37)) has pronounced maxima at Cherenkov frequencies, i.e. it has the same characteristic features as the incident field (3).

First of all, let us consider the asymptotic behavior of the sum $I^{(i0)}(\rho,z) + I_\beta^{(2)}(\rho,z)$ that coincides with the Fourier harmonic of the full field up to a multiplier in the region "2" in the absence of dielectric filling of the waveguide (i.e., when the charge escapes from the vacuum waveguide). Figure 2 shows the dependences of the modulus of this value in the far-field zone ($k_0 R \gg 1$) at $\gamma = 20$ and relatively small angles θ ($\theta \sim \theta_\beta$). The frequency ω is to be equal to the first Cherenkov frequency ω_1^{CR} for certainty, but there is no strong dependence on the proximity (or remoteness) of this frequency to the Cherenkov frequencies for the full field in the vacuum, which is quite natural. Mathematically, this is expressed in the fact that the value Q_m (34), which has a sharp

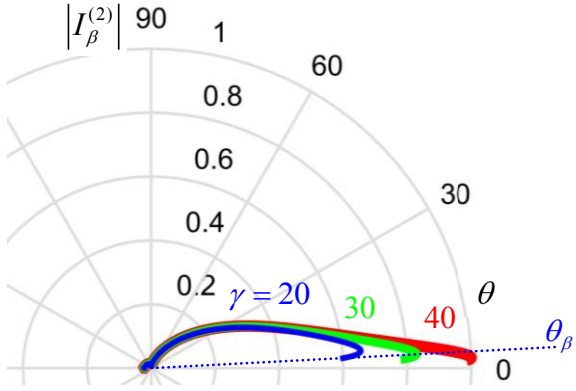

Fig. 3. (In color online) Normalized radiation patterns of a point charge when it escapes from the open end of a vacuum waveguide at different γ and angles in the range $\theta \in [\theta_\beta, \pi - \theta_\beta]$. The problem parameters are the same as in Fig. 2. The dotted line shows the angle θ_β for $\gamma = 20$

dependence on the frequency in the vicinity ω_m^{CR}, $m = 1,2\ldots$. is included only in the first term in (37). The blue lines are calculated using the uniform asymptotic formula (41), the red lines are calculated using the "non-uniform" asymptotic formula (47). It can be seen that at $k_0R = 5\gamma^2 = 2000$ ($\Lambda = 5$, the left graph in Fig. 2) the "non-uniform" asymptotics has a noticeable jump at $\theta = \theta_\beta$ and differs significantly from the uniform one in almost the entire range of angles presented on the graph. Mathematically, this is due to the fact that for $\Lambda = 5$ the argument of the function Q in (41) is not large enough at these viewing angles and the formula (46) is unapplicable. From a physical point of view, this means that the considered range of angles for given R lies in an area similar in essence to the penumbra region, where the spherical radiation wave is inseparable from the full field.

At $k_0R = 10\gamma^2 = 4000$ ($\Lambda = 10$, the middle graph in Fig. 2) the argument of the function Q in (41) is quite large at $\theta = \theta_\beta$ and larger angles, so the curves practically coincide at $\theta \geq \theta_\beta$ (the jump at $\theta = \theta_\beta$ als becomes insignificant), but there are still noticeable differences at $\theta < \theta_\beta$. Finally, at $\Lambda = 19$ (the right graph in Fig. 2) the curves practically coincide in the entire range of angles presented, including at $\theta = \theta_{min}$.

However, the range of angles at which (47) is an asymptotic of the original integral (39) is limited in the area of small angles by an additional inequality $\theta \gg \theta_{min}$. At $\gamma \gg 1$ the angle $\theta_\beta \approx \gamma^{-1}$ and therefore at $k_0R \geq 10\gamma^2$ satisfies this additional inequality, since at the same time $\theta_{min} \leq (\sqrt{10}\gamma)^{-1}$. Therefore for $\theta \geq \theta_\beta$ and $R \geq 10\gamma^2/k_0$, formula (47) describes the asymptotics of the integral (39), and

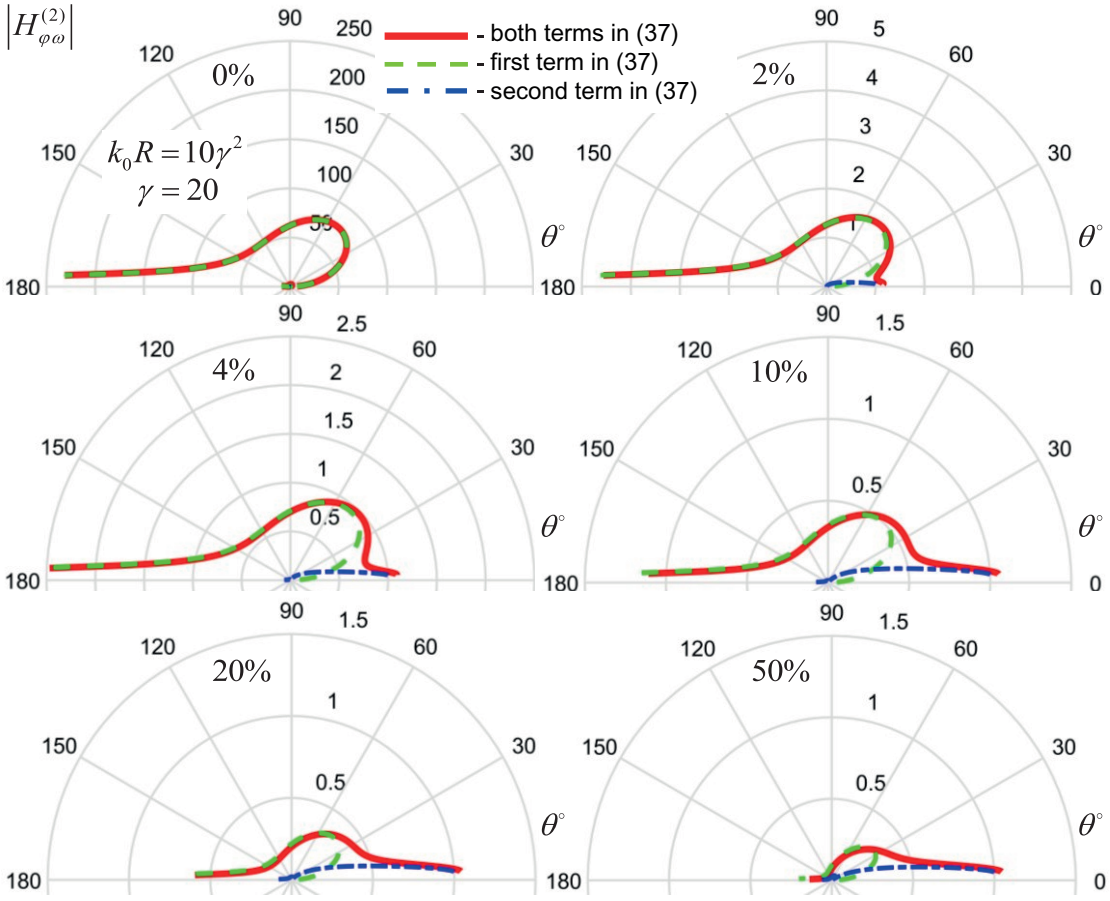

Fig. 4. (In color online) Radiation patterns of a point charge when it escapes from the open end of a waveguide with dilectric filling at $\gamma = 20$ and $R = 10\gamma^2 / k_0$ in the range of angles $\theta \in [\theta_\beta, \pi - \theta_\beta]$ at frequencies shifted from the first Cherenkov frequency ω_1^{CR} by a fraction of the difference $\omega_2^{CR} - \omega_1^{CR}$, indicated as a percentage on each graph. The solid (red) line is calculated according to the formula (37), the green (dotted) line is the contribution of the first term of (37), the blue (dashed) line is the contribution of the second term of (37). The curves are normalized to the maximum of the blue (dashed) line. The other parameters are the same as in Fig. 2, $\omega_2^{CR} \approx 2\pi \cdot 109.9$ GHz

the second term in this formula describes the asymptotics of the sum $I^{(i0)}(\rho, z) + I^{(2)}_{\beta}(\rho, z)$, i.e., up to a multiplier— the asymptotics of the Fourier harmonic of the full field in the vacuum case. In this range of angles and distances, the full field is represented only by a spherical wave of "vacuum" diffraction radiation, we can talk about the directional pattern of this radiation, and the self field of the charge is insignificant, since the jump in the curves of Fig. 2 associated with this field is negligible.

Fig. 3 shows normalized directional patterns of diffraction radiation at the open end of a vacuum waveguide (i.e., "vacuum" diffraction radiation) at different γ angles in the range $\theta \in [\theta_{\beta}, \pi - \theta_{\beta}]$ at the frequency of the first "Cherenkov mode". These diagrams are determined by the multiplier for the $\exp(ik_0 R) / R$ of the second term in (47). It can be seen that with growth of γ within the selected limits, the diagram practically does not change its shape, but the size of the main lobe increases.

Next, radiation in the presence of dielectric filling of the waveguide will be considered. Figure 4 shows radiation patterns in the far-field zone ($\pi - \theta_{\beta} \geq \theta \geq \theta_{\beta}$, $R = 10\gamma^2 / k_0$), calculated using the general formula (37), taking into account the asymptotics of the integral $I^{(2)}_m(\rho, z)$ in the form of a spherical wave (40) and the asymptotics of the integral $I^{(2)}_{\beta}(\rho, z)$ in the form of a spherical wave (47) (the second term). The solid (red) line corresponds to the full field, i.e. both terms in (37) are taken into account, the dotted (green) line corresponds to the first term in (37) (sum over m), the dashed (blue) line corresponds to the second term in (37). The curves are normalized to the maximum of the dashed line, i.e. to the maximum of diffraction radiation in the vacuum case. The frequency increases from graph to graph: in the upper left graph (marked "0%") the frequency is equal to ω_1^{CR}, then each graph shows an increase to ω_1^{CR} as a a percentage of the difference $\omega_2^{CR} - \omega_1^{CR}$.

Exactly at the Cherenkov frequency "vacuum" diffraction radiation is negligible (the dotted line is practically not visible on the graph "0%") and the radiation field is completely determined by the first term in the formula (37), radiation at small angles ("forward") is practically absent, there is strong "backward" radiation, i.e. at angles close to $\pi - \theta_{\beta}$. Note that significant radiation in the direction

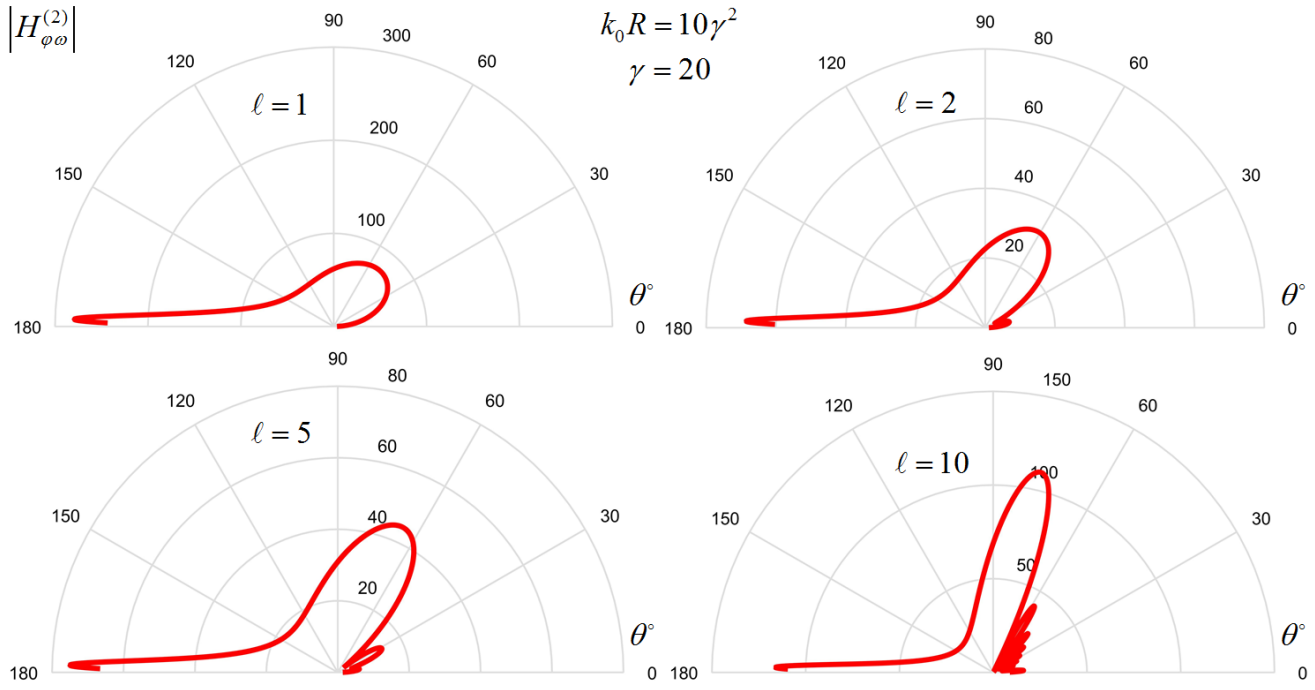

Fig. 5. Radiation patterns of a point charge when it escapes from the open end of a waveguide with dilectric filling at $\gamma = 20$, $R = 10\gamma^2 / k_0$ atthe Cherenkov frequency with a number $l = 1,2,5,10$ (the number is indicated on each graph) in the angle range $\theta \in [\theta_{\beta}, \pi - \theta_{\beta}]$. The curves are calculated according to formula (37) and normalized to the maximum of the second term in this formula. The task parameters are the same as in Fig. 4, $\omega_5^{CR} \approx 2\pi \cdot 297.2$ GHz, $\omega_{10}^{CR} \approx 2\pi \cdot 609.8$ GHz

of a small angle with the wall of the waveguide also occurs when the waveguide is excited by the TM mode [33, 28]. With increasing frequency (additive 2-10%), "vacuum" diffraction radiation begins to affect at small angles $\theta \sim \theta_\beta$, and with an addition of 20% it exceeds the "backward" radiation due to the first term in (37). At the same time, the radiation in other directions (other than "forward" and "backward") is significantly less. Finally, with an addition of 50%, "vacuum" diffraction radiation practically determines the total radiation.

Fig. 4 shows diagrams of radiation at Cherenkov frequencies with numbers $l = 1,2,5,10$, the curves are normalized to the maximum of "vacuum" diffraction radiation (it is not represented itself due to its negligible smallness, as can be seen from the normalization). It is also seen that with an increase in the number of the Cherenkov mode, the angle of maximum radiation into the forward half-space increases and the width of the corresponding main lobe decreases. At small l, the "backward" radiation is very strong, with an increase in the mode number its role decreases. At the same time, at $l \geq 2$ there are weak side lobes, the presence of which is associated with the radiation of propagating modes, the number of which is different from l.

4. CONCLUSION

This paper presents a rigorous solution to the problem of diffraction radiation of a uniformly moving point charge at the open end of a circular waveguide with a uniform dielectric filling. The solution consists of two components. The first component is diffraction radiation at the open end of the waveguide without dielectric filling, the so—called "vacuum" diffraction radiation. The second component can be interpreted as transition radiation at the dielectric-vacuum interface limited by the edges of the waveguide. At the Vavilov – Cherenkov radiation frequencies (they satisfy the condition $as = j_{0m}$, $m = 1,2\ldots$) the first component is negligible, and the radiation pattern is determined by the second component, as a rule it has a pronounced main lobe at an observation angle significantly larger than zero. Away from the Cherenkov frequencies, the first component dominates and forms a directional pattern with a narrow lobe in the vicinity of the axis of the structure (the corresponding maximum angle is equal in order of magnitude to the inverse Lorentz factor).

Note that from the point of view of practical applications described in the Introduction, it would be necessary to investigate a more realistic structure having a vacuum channel on the axis for an unobstructed charge passage. The approximation made about the uniformity of the dielectric filling is mainly due to considerations of the maximum possible simplicity and clarity of presentation. The problem solved in this paper is a necessary first step towards solving more complex problems, for example, the problem of diffraction radiation at the open end of a waveguide with a vacuum channel and a dielectric layer. The presented method can be applied without fundamental difficulties both to the described two-layer structure and to more multilayer structures in the same way as it was done in our works [28, 29, 37], where problems without an external source with excitation in the form of a waveguide mode were considered.

FUNDING

The study was carried out with the financial support of the Russian Science Foundation (Project 18-72-10137).

REFERENCES

1. B. M. Bolotovskii and G. V. Voskresenskii, *Diffraction radiation*, Usp. Fiz. Nauk, **88**, 209 (1966).
2. B. M. Bolotovskii and E. A. Galst'yan, *Diffraction and diffraction radiation*, Usp. Fiz. Nauk, **170**, 809 (2000).
3. S. Kheifets, L. Palumbo and V. G. Vaccaro, *Electromagnetic fields scattered by a charge moving on the axis of a semi-infinite circular waveguide*: *Radiation spectrum and longitudinal impedance*, IEEE Trans. Nucl. Science, **34**, 1094 (1987).

4. A. V. Tyukhtin, *Self-acceleration of a charge traveling into a waveguide*, Phys. Rev. ST Accel. Beams, **17**, 021303 (2014).
5. S. N. Galyamin, A. V. Tyukhtin, V. V. Vorobev, A. A. Grigoreva and A. Aryshev, *Bunch imaging at the open end of an embedded circular waveguide*, IEEE Trans. Microwave Theory Techn., **66**, 2100 (2018).
6. D. V. Karlovets and A. P. Potylitsyn, *On the theory of diffraction radiation*, Journal of Experimental and Theoretical Physics, **107**, 755 (2008).
7. D. Karlovets and A. Potylitsyn, *Generalized surface current method in the macroscopic theory of diffraction radiation*, Physics Letters A, **373**, 1988 (2009).
8. A. Potylitsyn, M. I. Ryazanov, M. N. Strikhanov and A. A. Tishchenko, *Diffraction Radiation from Relativistic Particles*, Springer Tracts in Modern Physics, Vol. 239 (Springer-Verlag Berlin Heidelberg, 2011).
9. M. Ivanyan, A. Grigoryan, A. Tsakanian and V. Tsakanov, *Wakefield radiation from the open end of an internally coated metallic tube*, Phys. Rev. ST Accel. Beams, **17**, 074701 (2014).
10. A. M. Altmark, A. D. Kanareykin and I. L. Sheinman, *Tunable wakefield dielectric-filled accelerating structure*, Tech. Phys., **50**, 87 (2005).
11. E. A. Nanni, W. R. Huang, K.-H. Hong, K. Ravi, A. Fallahi, G. Moriena, R. J. Dwayne Miller and F. X. Kärtner, *Terahertz-driven linear electron acceleration*, Nature Communications, **6**, 8486 (2015).
12. B. D. O'Shea, G. Andonian, S. Barber, K. Fitzmorris, S. Hakimi, J. Harrison, P. D. Hoang, M. J. Hogan, B. Naranjo, O. B. Williams, V. Yakimenko and J. Rosenzweig, *Observation of acceleration and deceleration in gigaelectron-volt-per-metre gradient dielectric wakefield accelerators*, Nature Communications, **7**, 12763 (2016).
13. D. Wang, X. Su,L. Yan, Y. Du, Q. Tian, Y. Liang, L. Niu, W. Huang, W. Gai, C. Tang and S. Antipov, *Phase control with two-beam interferometry method in a terahertz dielectric wakefield accelerator*, Appl. Phys. Lett., **111**, 174102 (2017).
14. C. Jing, S. Antipov, M. Conde, W. Gai, G. Ha, W. Liu, N. Neveu, J. Power, J. Qiu, J. Shi, D. Wang and E. Wisniewski, *Electron acceleration through two successive electron beam driven wakefield acceleration stages*, Nucl. Instr. Meth. Phys. Res. A, **898**, 72 (2018).
15. M. T. Hibberd, A. L. Healy, D. S. Lake, V. Georgiadis, E. J. H. Smith, O. J. Finlay, T. H. Pacey, J. K. Jones, Y. Saveliev, D. A. Walsh, E. W. Snedden, R. B. Appleby, G. Burt, D. M. Graham and S. P. Jamison, *Acceleration of relativistic beams using laser-generated terahertz pulses*, Nature Photonics, **14**, 755 (2020).
16. H. Tang, L. Zhao, P. Zhu, X. Zou, J. Qi, Y. Cheng, J. Qiu, X. Hu, W. Song, D. Xiang, and J. Zhang, *Stable and scalable multistage terahertz-driven particle accelerator*, Phys. Rev. Lett., **127**, 074801 (2021).
17. S. N. Galyamin, A. V. Tyukhtin, S. Antipov, and S. S. Baturin, *Terahertz radiation from an ultra-relativistic charge exiting the open end of a waveguide with a dielectric layer*, Opt. Express, **22**, 8902 (2014).
18. D. Wang, X. Su, Y. Du, Q. Tian, Y. Liang, L. Niu, W. Huang, W. Gai, L. Yan, C. Tang, and S. Antipov, *Non-perturbing THz generation at the Tsinghua university accelerator laboratory 31 MeV electron beamline*, Review of Scientific Instruments, **89**, 093301 (2018).
19. L. Zhao, H. Tang, C. Lu, T. Jiang, P. Zhu, L. Hu, W. Song, H. Wang, J. Qiu, C. Jing, S. Antipov, D. Xiang, and J. Zhang, *Femtosecond relativistic electron beam with reduced timing jitter from Thz driven beam compression*, Phys. Rev. Lett., **124**, 054802 (2020).
20. S. Jiang, W. Li, Z. He, Q. Jia, and L. Wang, *Intrinsically reducing divergence angle of Cherenkov radiation from dielectric capillary*, Opt. Lett., **45**, 5416 (2020).
21. G. Voskresenskii and S. Zhurav, Radiotekhnika i Electronika, **12**, 2608 (1976).
22. G. Voskresenskii and S. Zhurav, Radiotekhnika i Electronika, **23**, 2505 (1978).
23. S. Koshikawa and K. Kobayashi, *Diffraction by a terminated semi-infinite parallel-plate waveguide with three-layer material loading*, IEEE Transactions on Antennas and Propagation, **45**, 949 (1997).
24. Y. Hamеs and I. H. Tayyar, *Radiation from dielectric-filled thick-walled parallel-plate waveguide junction loaded with a dielectric half-plane*, Electromagnetics, **25**, 245 (2005).
25. R. Mittra and S. W. Lee, *Analytical Techniques in the Theory of Guided Waves*, (Macmillian, 1971).
26. S. N. Galyamin, A. V. Tyukhtin, V. V. Vorobev, A. A. Grigoreva and A. S. Aryshev, *Cherenkov radiation of a charge exiting open-ended waveguide with dielectric filling*, Phys. Rev. Accel. Beams, **22**, 012801 (2019).
27. S. N. Galyamin, A. V. Tyukhtin and V. V. Vorobev, *Radiation from open ended waveguide with dielectric loading*, Nuclear Instr. Meth. Phys. Res. B, **402**, 144 (2017).
28. S. N. Galyamin, V. V. Vorobev and A. V. Tyukhtin, *Diffraction at the open-ended dielectric-loaded circular waveguide*: *Rigorous approach*, IEEE Trans. Microwave Theory Techn., **69**, 2429 (2021).
29. S. N. Galyamin and V. V. Vorobev, *Diffraction at the open end of dielectric-lined circular waveguide*, IEEE Trans. Microwave Theory and Techn., **70**, 3087 (2022).

30. I. H. Tayyar and A. Buyukaksoy, *A Wiener-Hopf analysis of the coaxial waveguide radiator*, 2011 International Conference on Electromagnetics in Advanced Applications (2011), pp. 580–583.

31. L. Weinstein, *The Theory of Diffraction and the Factorization Method*: *generalized Wiener-Hopf Technique*, Golem Series in Electromagnetics, V. 3 (Golem Press, 1969).

32. L. B. Felsen and N. Marcuvitz, *Radiation and Scattering of Waves* (Wiley Interscience, New Jersey, 2003).

33. B.M. Bolotovskii, D.M. Sedraky'an, Radiation of a particle from an open end of a waveguide, Proceedings of Academy of Sciences of Armenian SSR, 17, 119 (1964).

34. N. Sei and T. Takahashi, *First demonstration of coherent Cherenkov radiation matched to circular plane wave*, Scientific Reports, **7**, 17440 (2017).

35. P. Karataev, K. Fedorov, G. Naumenko, K. Popov, A. Potylitsyn, and A. Vukolov, *Ultra-monochromatic far-infrared Cherenkov diffraction radiation in a super-radiant regime*, Scientific Reports, **10**, 20961 (2020).

36. R. Kieffer, L. Bartnik, M. Bergamaschi, V. V. Bleko, M. Billing, L. Bobb, J. Conway, M. Forster, P. Karataev, A. S. Konkov, R. O. Jones, T. Lefevre, J. S. Markova, S. Mazzoni, Y. Padilla Fuentes, A. P. Potylitsyn, J. Shanks, and S. Wang, *Direct observation of incoherent Cherenkov diffraction radiation in the visible range*, Phys. Rev. Lett., **121**, 054802 (2018).

37. S. N. Galyamin, *Cherenkov Wakefield Radiation from an Open End of a Three-Layer Dielectric Capillary*, arXiv.org. 2022. URL: https://doi.org/10.48550/arXiv.2205.03986.